

A realistic heat bath:  
theory and application to kink-antikink dynamics

A. Krasnitz\* and Robertus Potting\*\*

*Physics Department*

*Indiana University*

*Bloomington, Indiana 47405*

*and*

*\*Interdisciplinary Project Center for Supercomputing*

*Eidgenössische Technische Hochschule-Zentrum*

*CH-8092 Zurich, Switzerland*

*\*\*Universidade do Algarve*

*Unidade de Ciências Exactas e Humanas*

*Campus de Gambelas, 8000 Faro, Portugal*

We propose a new method of studying a real-time canonical evolution of field-theoretic systems with boundary coupling to a realistic heat bath. In the free-field case the method is equivalent to an infinite extension of the system beyond the boundary, while in the interacting case the extension of the system is done in linear approximation. We use this technique to study kink-antikink dynamics in  $\varphi^4$  field theory in 1+1 dimensions.

## I. INTRODUCTION

There is a growing interest in transitions over energy barriers in field theories at finite temperature. The motivation comes from high-energy physics and cosmology (*e.g.*, baryon-number violating sphaleron transitions in electroweak theory [1]- [6]), as well as from condensed-matter physics (*e.g.*, current-reducing fluctuations in one-dimensional superconductors [7]). Such thermally induced transitions usually involve collective excitations like kink-antikink pairs or sphalerons, and therefore occur in a nonlinear setting. The nonlinearity, in turn, often renders analytic techniques useless, forcing one to resort to numerical (lattice) methods. On the other hand, many questions of interest can be answered by considering the classical regime in which the temperature is much larger than the energies of the field quanta at the scale of a relevant collective excitation [6].

A fundamental quantity of interest is the corresponding transition rate. Unlike static observables, it cannot be determined from a given canonical ensemble of field configurations. Instead, one must follow a real-time evolution of the field-theoretic system in the heat bath. Obviously, the rate would depend on the properties of the heat bath and its coupling to the system. This was indeed confirmed by recent numerical studies [3] [4], in which the heat bath was implemented through Langevin equation. In most naturally occurring situations a system interacts with its environment through the boundaries, and the environment is an infinite extension of the system itself. This consideration dictates our choice of a heat bath in this work. Ideally, the heat bath we model should possess two main properties: (*a*) waves traveling through the boundary out of the system should be completely absorbed, as if there were no boundary and the system had an infinite extension; and (*b*) the waves traveling into the system should be thermally distributed. Our construction of a heat bath ensures these two properties in the free-field case, while for an interacting field they hold in the linear approximation. The similarity between our linearized heat bath and the true extension of the interacting system becomes better with decreasing temperature. Note that the standard Langevin dynamics, imposed either in the bulk of the system or at the boundary [11], will

not lead to the properties  $a$  and  $b$ .

While the idea of mimicking a natural heat bath is very generally applicable, we restrict ourselves in this article to the case of a scalar field in one spatial dimension. In Section II we derive the boundary force exerted by the heat bath on this one-dimensional system. Next, we show in Section III how our construction of the realistic heat bath can be implemented numerically. As an example, in Section IV we apply our technique to study kink-antikink pair nucleation in  $\varphi^4$  theory, a subject that has been extensively investigated by other methods [4]- [6]. We summarize and discuss our results in Section V.

## II. THE METHOD

Consider a lattice system consisting of a (possibly self-interacting) scalar field  $\varphi_n$ , with a minimum of its potential  $V(\varphi)$  at  $\varphi = v$  and mass  $m$  corresponding to that minimum. For definiteness, let it reside on the  $n \leq 0$  sites of a one-dimensional chain, and be coupled to a heat bath at  $n = 0$ . Let the heat bath be a free massive scalar field system on the positive  $n$  sites with equation of motion (the lattice spacing is  $a$ )

$$\ddot{\Phi}_n - \frac{\Phi_{n+1} + \Phi_{n-1} - 2\Phi_n}{a^2} + m^2\Phi_n = 0 \quad (1)$$

for  $n \geq 1$  and boundary condition

$$\Phi_0(t) = \varphi_0(t) - v = f(t). \quad (2)$$

Given the solution  $\Phi_n(t)$ , there will be a reaction force exerted by the heat bath on the system:

$$F(t) = (\Phi_1 - \Phi_0)/a^2. \quad (3)$$

The  $\Phi_0$  contribution to  $F(t)$  is a harmonic force. The  $\Phi_1$  contribution, called  $f_{\text{mem}}$  (the memory force) in the following, is, as we shall see immediately, a response of a more general nature. As the heat bath is a free field system, this response should be linear. Furthermore,

it should causally depend on  $f(t)$ . In other words, there exists a response function  $\chi(t)$  ( $t > 0$ ) such that

$$f_{\text{mem}}(t) = \int_{-\infty}^t f(t')\chi(t-t')dt'. \quad (4)$$

In order to determine  $\chi(t)$  let us take  $f(t) = e^{st}$ . It follows from Eq. 1 that  $\Phi_n(t) = \exp(st - k_s a n)$ , with

$$k_s = \frac{2}{a} \operatorname{arcsinh} \left( \frac{a}{2} \sqrt{s^2 + m^2} \right). \quad (5)$$

Using Eq. 3 we then find that  $\chi(t)$  should satisfy

$$\frac{1}{a^2} e^{st - k_s a} = \int_{-\infty}^t e^{st'} \chi(t-t') dt' = e^{st} (\mathcal{L}\chi)(s), \quad (6)$$

where  $\mathcal{L}$  denotes the Laplace transform. It follows that

$$\begin{aligned} \chi(t) &= a^{-2} \mathcal{L}^{-1}(e^{-ak_s}) \\ &= \frac{1}{a^2} \mathcal{L}^{-1} \left( (\sqrt{1+y} - \sqrt{y})^2 \right) \quad \text{with } y = a^2(s^2 + m^2)/4. \end{aligned} \quad (7)$$

The integral in Eq. 4 is most easily computed in Fourier space. We define  $\tilde{f}_t(\omega) = \int_{-\infty}^t e^{i\omega(t'-t)} f(t') dt'$  and  $\tilde{\chi}(\omega) = \int_{-\infty}^{\infty} e^{i\omega t} \chi(t) dt$ , where we are free to take any extension of  $\chi(t)$  for  $t < 0$ . Then it follows from the convolution theorem that

$$f_{\text{mem}}(t) = \frac{1}{2\pi} \int \tilde{\chi}(\omega) \tilde{f}_t(\omega) d\omega. \quad (8)$$

For numerical purposes it is best to extend  $\chi(t)$  to  $t < 0$  such that  $\tilde{\chi}(\omega)$  vanishes outside a finite interval. To this end we choose  $\chi(t) = -\chi(-t)$ , so  $\tilde{\chi}(\omega)$  becomes purely imaginary (essentially the sine transform). The latter can be obtained immediately from the Laplace transform (Eq. 7) by the  $\pi/2$  rotation of  $s$  in the complex plane; taking the imaginary part then gives

$$\tilde{\chi}(\omega) = i \operatorname{sign}(\omega) \sqrt{(\omega^2 - m^2)(1 + a^2(m^2 - \omega^2)/4)} \quad (9)$$

for frequencies  $m < |\omega| < \sqrt{m^2 + 4/a^2}$  corresponding to propagating modes and  $\tilde{\chi}(\omega) = 0$  outside this range.

We expect the heat bath response to be finite for any bounded  $f(t)$  (Eq. 4). If so,  $\chi(t)$  must decay sufficiently rapidly in the distant future. This indeed is the case: using Eq. 9 and performing the inverse Fourier transform we find in the saddle-point approximation  $\chi(t) \propto t^{-3/2} \sin(mt + \pi/4)$  as  $t \rightarrow \infty$ .

The dissipation by the heat bath can equivalently be described by a linear response to the momentum  $\pi_0$  at the boundary, rather than the field. Explicitly, it follows from Eq. 4 that

$$f_{\text{mem}}(t) = - \int_{-\infty}^t \psi(t-t') \pi_0(t') dt', \quad (10)$$

where  $\psi(t) = \int_0^t \chi(t') dt'$  or, equivalently,  $(\mathcal{L}\psi)(s) = s^{-1}(\mathcal{L}\chi)(s)$ , so that

$$\tilde{\psi}(\omega) = i\omega^{-1} \tilde{\chi}(\omega). \quad (11)$$

We now turn to the second contribution to the boundary force, the random force  $f_{\text{ran}}$ . It is a Gaussian random variable whose properties are defined by its time autocorrelation  $C(\tau) = \langle f_{\text{ran}}(t) f_{\text{ran}}(t + \tau) \rangle$ . These are most easily determined through the fluctuation-dissipation theorem, stating

$$C(\tau) = \theta \psi(|\tau|) \quad (12)$$

( $\theta$  denotes the temperature). Numerical implementation of  $f_{\text{ran}}$  amounts to generating Gaussian noise with this autocorrelation function.

One can check explicitly that the time correlation function of the total boundary force  $F + f_{\text{ran}}$  is equal to the average of  $((\Phi_n(0) - \Phi_{n-1}(0))(\Phi_n(t) - \Phi_{n-1}(t))/a^4$  for a canonical ensemble, calculated for an infinitely extended free field. This is to be expected, as  $(\Phi_n - \Phi_{n-1})/a^2$  represents the force between neighboring sites.

We conclude this section by discussing the continuum limit of the heat bath response. Obviously,  $F(t)$  diverges as  $a \rightarrow 0$ . Instead,  $aF(t)$  is a well-behaved quantity whose limit is simply  $\partial_x \Phi(x=0, t)$ , where  $x$  is the continuum spatial coordinate. In other words, if we prescribe the boundary field motion, the heat bath response will determine the boundary

field spatial derivative in such a way that the waves traveling out of the system will not be reflected at the boundary. The corresponding response function is found following steps analogous to Eq. 4–Eq. 7. We write down the continuum equations of motion

$$\ddot{\Phi} - \partial_x^2 \Phi + m^2 \Phi = 0 \quad (x > 0) \quad (13)$$

together with the boundary condition  $\Phi(0, t) = f(t)$  and require

$$\partial_x \Phi(0, t) = \int_{-\infty}^t f(t') \chi_c(t - t') dt'. \quad (14)$$

Taking  $f(t) = \exp(st)$  then yields  $\chi_c(t) = \mathcal{L}^{-1}(\sqrt{s^2 + m^2})$ , or  $\chi_c(t) = \delta'(t - 0_+) + mt^{-1} J_1(mt)$ .

It is an easy exercise to verify that the same result is obtained by first computing the response function for the lattice boundary field derivative and then taking the limit  $a \rightarrow 0$ .

### III. NUMERICAL IMPLEMENTATION

Our numerical implementation of the boundary force is as follows. The memory force  $f_{\text{mem}}(t)$  is computed using Eq. 8, that is, in Fourier space. The function  $\tilde{\chi}(\omega)$  is given by Eq. 9. In practice, the integral Eq. 8 is replaced by a finite sum over discrete values of  $\omega$ , separated by an increment  $\Delta\omega$ . As a result, the response function  $\chi(t)$  becomes periodic in  $t$  with a period  $2\pi/\Delta\omega$ . Beyond  $t = 2\pi/\Delta\omega$  our approximation of  $\chi(t)$  is incorrect, and the lower limit of integration in Eq. 4 should be cut off. We achieve this by changing the definition of  $\tilde{f}_t(\omega)$  to

$$\tilde{f}_t(\omega) = \int_{t-T}^t e^{i\omega(t'-t)} f(t') dt', \quad (15)$$

where  $T < 2\pi/\Delta\omega$ . At the same time,  $T$  should be large enough so the discarded part of the integral Eq. 8 is negligible. With the new definition,  $\tilde{f}_t(\omega)$  satisfies the equation of motion

$$\dot{\tilde{f}}_t(\omega) = -i\omega \tilde{f}_t(\omega) + f(t) - e^{-i\omega T} f(t - T). \quad (16)$$

The random force  $f_{\text{ran}}$  is computed by convolving white noise of unit power spectrum with a function  $R(t)$  whose Fourier image is given by  $\sqrt{\tilde{C}(\omega)}$ , where  $\tilde{C}$  is the Fourier transform of  $C(t)$  given by Eq. 12 [9]. This can be done very efficiently using FFT algorithms.

With both ingredients of the boundary force in place, we can now write down and integrate the equations of motion for the one-dimensional system immersed in the heat bath. These equations have the standard form

$$\ddot{\varphi}_n - \frac{\varphi_{n+1} + \varphi_{n-1} - 2\varphi_n}{a^2} - V'(\varphi_n) = 0 \quad (17)$$

in the bulk of the system, but should be modified at the boundaries. For example, at the left boundary we have

$$\ddot{\varphi}_0 - \frac{\varphi_1 - 2\varphi_0}{a^2} - V'(\varphi_0) = f_{\text{mem,left}} + f_{\text{ran,left}}, \quad (18)$$

and the right-boundary analog is obvious. The system of equations of motion for the field is supplemented by Eq. 16 governing the evolution of the memory forces at both boundaries.

We integrate equations 17, 18, and 16 using the second-order Runge-Kutta algorithm. While this way of updating  $\tilde{f}_t(\omega)$  is efficient compared to computation of the full integral Eq. 15, it is not accurate enough to maintain correct phases of  $\tilde{f}_t(\omega)$  for times much longer than  $2\pi/\Delta\omega$ . To ensure stability, we therefore adjust the values of  $\tilde{f}_t(\omega)$  by computing Eq. 15 every  $T$  time units.

We have tested the action of  $f_{\text{mem}}$  by evolving an initially hot system with  $f_{\text{ran}}$  omitted. This corresponds to cooling in the zero-temperature heat bath. The resulting evolution is very similar to that of a benchmark run where we substitute for the heat bath a real cold free-field system with large volume. This similarity holds separately for every momentum mode. The method allows cooling the system to at least  $10^{-5}$  times its original temperature. Cooling curves for a system with a real and with a simulated heat bath are shown in Figure 1.

We then turned  $f_{\text{ran}}$  on and tested it by heating a cold field configuration to a prescribed temperature. Again it compared well, mode by mode, with a benchmark run, in which we coupled a cold system to a large real heat bath whose temperature the system eventually reached (let us stress that using the real heat bath is much more costly in terms of CPU time). Both heating curves are shown in Figure 2.

Finally, we have shown numerically the self-consistency of our method by comparing the motion of the endpoint field to that in the middle of the system [10]. As Figure 3 shows, the autocorrelation curves of the two fields are very close to each other, meaning that the simulated free-field heat bath closely approximates the real one.

#### IV. KINK-ANTI-KINK DYNAMICS IN 1+1 DIMENSIONS

We have applied our method to investigate kink-antikink dynamics of  $\varphi^4$  theory whose Lagrangian is

$$L = \int dx \left( \frac{1}{2} (\dot{\varphi}^2 - (\partial_x \varphi)^2) - \frac{1}{4} (\varphi^2 - 1)^2 \right) \quad (19)$$

in suitably chosen units [6]. Kinks and antikinks are finite-energy solutions of the equations of motion interpolating between the vacuum values of the field  $\varphi = \pm 1$ . Explicit functional form of the static kink is  $\varphi_{\pm}(x) = \tanh(\pm \frac{x}{\sqrt{2}})$ . The spatial extension of a kink is approximately  $\sqrt{2}$ , and the kink mass is  $M = \sqrt{8/9}$ .

Following [4], we chose a system of  $N = 400$  sites with lattice spacing  $a = 0.5$ . The simulations were performed at seven values of inverse temperature  $\beta$  between 3.0 and 6.0. Our Runge-Kutta time step was 0.005. For each value of the temperature we started from an ordered system and warmed it up for 2500 time units followed by  $2 \times 10^5$  time units over which we measured the number of kinks  $n$ . For the latter we used the same definition as in [4]: the number of zeros in a field configuration smoothed over the physical distance of  $\Delta L = 5$ .

The average kink number  $\langle n \rangle$  at a given temperature should not depend on the properties of a heat bath. Our measurements of this observable, shown in Figure 4, are indeed close to those of [4]. Note, however, that our measurement errors are much larger, especially for low temperatures, even though our data sample is as big as in [4]. We estimated the errors using a jackknife method with the block size varying over a very long range; we are therefore confident that the autocorrelation of our data is properly taken into account. Moreover, we



studied a microcanonical evolution of our system at the energy roughly corresponding to  $\beta = 4.5$ , with the error estimate similar to that of the corresponding canonical case.

The temperature dependence of  $\langle n \rangle$  may be interpreted in terms of the effective kink mass. Namely, one expects [8]

$$\langle n \rangle \propto \sqrt{\beta} \exp(-\beta M_{\text{eff}}). \quad (20)$$

It was found in earlier work that  $M_{\text{eff}} < M$ . It was also indicated that  $M_{\text{eff}}$  is temperature dependent [4], [5]. Both features find further evidence in our study. If we try to fit all our measurements of  $\langle n \rangle$  to Eq. 20 at once, an unacceptably low goodness-of-fit results. The situation improves dramatically if we exclude the highest-temperature point from the fit. We then find  $M_{\text{eff}} = 0.695 \pm 0.0095$ , or  $M_{\text{eff}} = (0.737 \pm 0.010)M$ , in good agreement with [4]. Alternatively, we can use pairs of consecutive values of  $\langle n \rangle$  to extract  $M_{\text{eff}}$ . The result, presented in Figure 5, shows the tendency of  $M_{\text{eff}}$  to decrease at higher temperatures, in agreement with findings of [4], [5].

Another interesting quantity we extract from the kink-antikink number time history is a kink lifetime, *i.e.* the autocorrelation time  $\tau$  of  $n$ . The latter is usually obtained by fitting the  $n$  autocorrelation function  $\langle (n(t) - \langle n \rangle)(n(0) - \langle n \rangle) \rangle$  to a single exponential of the form  $\exp(-t/\tau)$ . If the time history exhibits more than one time scale (as is the case for  $n$ ),  $\tau$  can only be given an average, or effective meaning. The existence of such multiple scales also makes a single-exponential fit to the autocorrelation function extremely difficult. A multiexponential fit to noisy data is not a practical possibility. We use an alternative way of determining  $\tau$ , closely related to the integral definition of the autocorrelation time. Namely, if  $\Delta t$  is a time interval between two consecutive measurements of  $n$ , we expect

$$\begin{aligned} w(N) &\equiv \langle (\sum_{i=0}^{N-1} n(i\Delta t) - N\langle n \rangle)^2 \rangle \\ &\approx \langle (n - \langle n \rangle)^2 \rangle \left[ \frac{N}{\tanh\left(\frac{\Delta t}{2\tau}\right)} - \frac{1}{2 \sinh^2\left(\frac{\Delta t}{2\tau}\right)} \right]. \end{aligned} \quad (21)$$

Obviously, for large  $N$   $w(N)$  approaches a random-walk behavior. For a given  $N$  we determine  $w(N)$  from our data set and solve Eq. 21 for  $\tau$ . For  $t \equiv N\Delta t \gg \tau$  the result

is approximately independent of  $N$ , and we take it as an estimate of the kink lifetime. A typical dependence of  $\tau$  on  $t$  is shown in Figure 6. Note that large values of  $t$  for which the plateau is reached indicate the existence of multiple time scales in the kink-antikink number fluctuations.

Unlike the exponential fit, this method also allows a well-defined error-estimating procedure for  $\tau$ . In particular, we apply the jackknife technique. Note that the lag values  $t$  used to determine  $\tau$  are of the order of 5000. This is to be compared to our  $n$  time history length of  $2 \times 10^5$ . We therefore only have a small effective number of independent measurements of  $\tau$ , and our error estimate cannot be very accurate. Conservatively we can expect the errors of  $\tau$  to be correct within a factor of 2. This might explain their inhomogeneous dependence on the temperature.

Kink-antikink pair nucleation can be viewed as a multidimensional analog of a particle escape over a barrier [2], [8], with the kink lifetime related to the effective barrier height  $B$  [4]:

$$\tau \propto \exp(\beta U), \quad (22)$$

where  $U = B - M_{\text{eff}}$ . From our data (Figure 7) we find  $U = 1.01 \pm 0.06 = (1.07 \pm 0.06)M$ , slightly higher than  $U = (0.85 \pm 0.15)M$  of [4], obtained by solving a low-viscosity Langevin equation. Both that value and ours are inconsistent with the naively expected  $B = 2M$ . More work is required to explain this discrepancy [12]. More importantly, however, our results show no exponential suppression of the kink-antikink pairs nucleation rate with growing temperature, in agreement with analytical predictions and earlier numerical work [2]- [6].

## V. CONCLUSIONS AND OUTLOOK

In this article we presented a method of modeling naturally occurring heat baths. While our presentation concentrated on a scalar field in one spatial dimension, the principles underlying our construction of a heat bath do not depend on the dimensionality or the field

content of a theory in question. In any case, one can determine the memory force exerted by a heat bath by studying the linear response of the latter to the field motion at the system boundary. The corresponding random component of the force may then be found using fluctuation-dissipation theorem. The only new feature to appear in dimensions higher than one is related to the connectedness of the boundary: the field motion at different points of the boundary will be correlated in a way consistent with causality. This is, however, a technical difficulty, not a conceptual one. The work on extending our method to other systems is currently in progress.

We have verified numerically that our simulated heat bath thermalizes correctly both linear and nonlinear systems. As an application, we considered the dynamics of kink-antikink pairs in  $\varphi^4$  theory. Our measurements of the kink density agree well with those obtained by solving Langevin equation, as one would expect for an equilibrium quantity independent of a heat bath implementation. The kink lifetimes we measure are close to those following from the low-viscosity Langevin dynamics. This is again to be expected for sufficiently large systems: as the system size grows, the influence of the boundary heat bath on the dynamics decreases. The Langevin analog would then be decreasing viscosity.

To conclude, we emphasize again an important advantage of our simulated heat bath over the Langevin method (including its zero-viscosity microcanonical limit): our heat bath is not arbitrarily chosen and involves no free parameters like viscosity. Rather, it is, to the best of our knowledge, the closest known approximation to a natural situation, in which open systems are immersed in a similar environment. The only physical (not numerical) approximation we make is linearization: our heat bath exchanges linear excitations (plane waves, or mesons) with the system, but not nonlinear ones (kinks, or baryons). Since we are only interested in pair creation and annihilation processes, the exchange of topological charge with the environment should have little impact on our results. It follows that we can approximately (the only approximation being linearization of the heat bath) identify our simulation time with the real physical one. The transition rates we measure have therefore direct physical meaning.

## ACKNOWLEDGMENTS

We are indebted to Ph. de Forcrand, to S. Gottlieb, and to A. Kovner for many interesting discussions and helpful suggestions. This work was supported by the US Department of Energy and by the Swiss Nationalfond.

## REFERENCES

- <sup>1</sup> For a review see, *e.g.*, A. D. Dolgov, Phys. Rep. **222**, 309 (1992).
- <sup>2</sup> M. Dine, O. Lechtenfeld, B. Sakita, W. Fischler, and J. Polchinski, Nucl. Phys. B **342**, 381 (1990).
- <sup>3</sup> A. I. Bochkarev and Ph. de Forcrand, "Nonperturbative evaluation of the diffusion rate in field theory at high temperatures", IPS Research Report No. 92-18, October 1992.
- <sup>4</sup> M. Alford, H. Feldman, and M. Gleiser, Phys. Rev. Lett. **68**, 1645 (1992).
- <sup>5</sup> A. I. Bochkarev and Ph. de Forcrand, Phys. Rev. Lett. **63**, 2337 (1989).
- <sup>6</sup> D. Grigoriev and V. Rubakov, Nucl. Phys. B **299**, 67 (1988).
- <sup>7</sup> N. Giordano, Phys. Rev. B **41**, 6350 (1990) and references therein.
- <sup>8</sup> P. Hänggi, F. Marchesoni, and P. Sodano, Phys. Rev. Lett. **60**, 2563 (1988); F. Marchesoni, *ibid* **64**, 2212 (1990).
- <sup>9</sup> In fact, the choice of phase for the Fourier transform of  $R(t)$  is arbitrary. There is a unique choice which would make  $R(t)$  causal. In the present work we choose zero phase for convenience.
- <sup>10</sup> We thank Ph. de Forcrand for suggesting this test.
- <sup>11</sup> Z. Rieder, J. L. Lebowitz, and E. Lieb, J. Math. Phys. **8**, 1073 (1967); U. Zürcher and P. Talkner, Phys. Rev. A **42**, 3267 (1990); *ibid*, 3278 (1990).
- <sup>12</sup> A word of caution is due regarding any attempt at numerical verification of analytical predictions for kink-antikink dynamics. Namely, both static and dynamical properties of the kink-antikink gas are sensitive to the way the kink-antikink number is defined, *i.e.* to the smearing length  $\Delta L$ . To check the  $\Delta L$  dependence of our results we determined  $\langle n \rangle$  and  $\tau$  at  $\beta = 3.0, 4.5$ , and  $6.0$  for a range of  $\Delta L$  values between  $0.5$  and  $5$ . Both  $M_{\text{eff}}$  and  $U$  evidently are  $\Delta L$ -dependent. For example,  $U$  varies from  $0.66$  to  $1.01$  for  $\Delta L$  in

that range. On the other hand, the analytical predictions do not take  $\Delta L$  into account at all, and can therefore only serve as a qualitative guide for interpreting numerical experiments.

## FIGURES

FIG. 1. Cooling curves for a free-field system ( $m = 0.5, a = 1, L = 100$ ) immersed in a simulated (squares) and real (solid line) zero-temperature heat baths.

FIG. 2. Heating curves for a free-field system ( $m = 0.5, a = 1, L = 100$ ) immersed in a simulated (squares) and real (solid line) heat baths. The equilibrium is reached at  $\theta = 1$ .

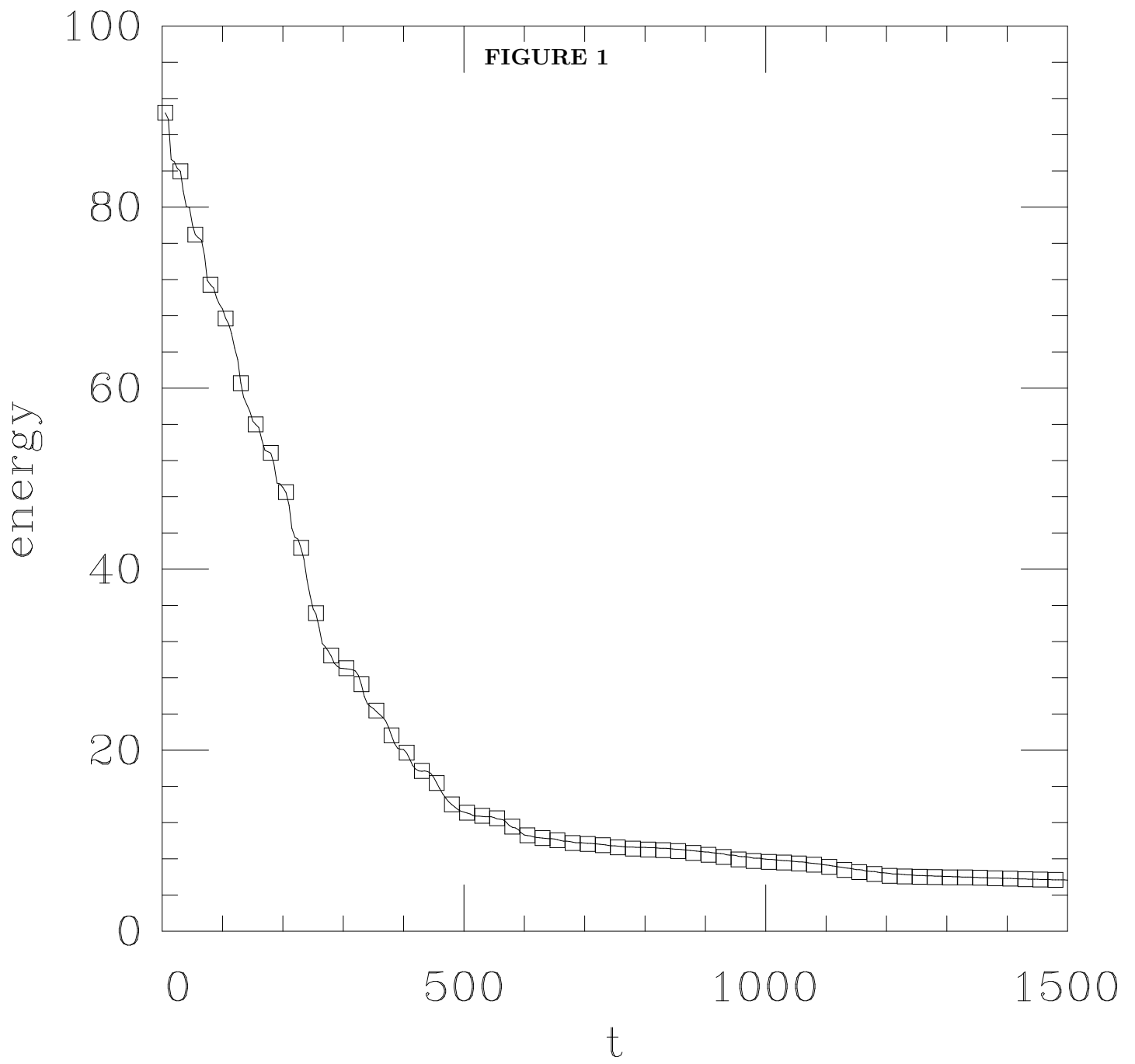
FIG. 3. Autocorrelation functions of the endpoint (solid line) and midpoint (squares) fields for a free-field system ( $m = 0.5, a = 1, L = 100$ ) at  $\theta = 1$ .

FIG. 4. Temperature dependence of the kink number (logarithmic scale). The solid line is a fit for  $M_{\text{eff}} = 0.737M$ .

FIG. 5. Temperature dependence of the kink effective mass obtained by fitting pairs of consecutive points from Figure 4 to Eq. 20. The inverse temperature  $\beta$  is that of a higher-temperature point in each pair.

FIG. 6. The kink number autocorrelation time  $\tau$  at  $\beta = 4$  determined from Eq. 21, plotted as a function of the lag  $N\Delta t$ .

FIG. 7. Temperature dependence of the kink lifetime (logarithmic scale). The solid line is a fit for  $U = 1.06M$ .





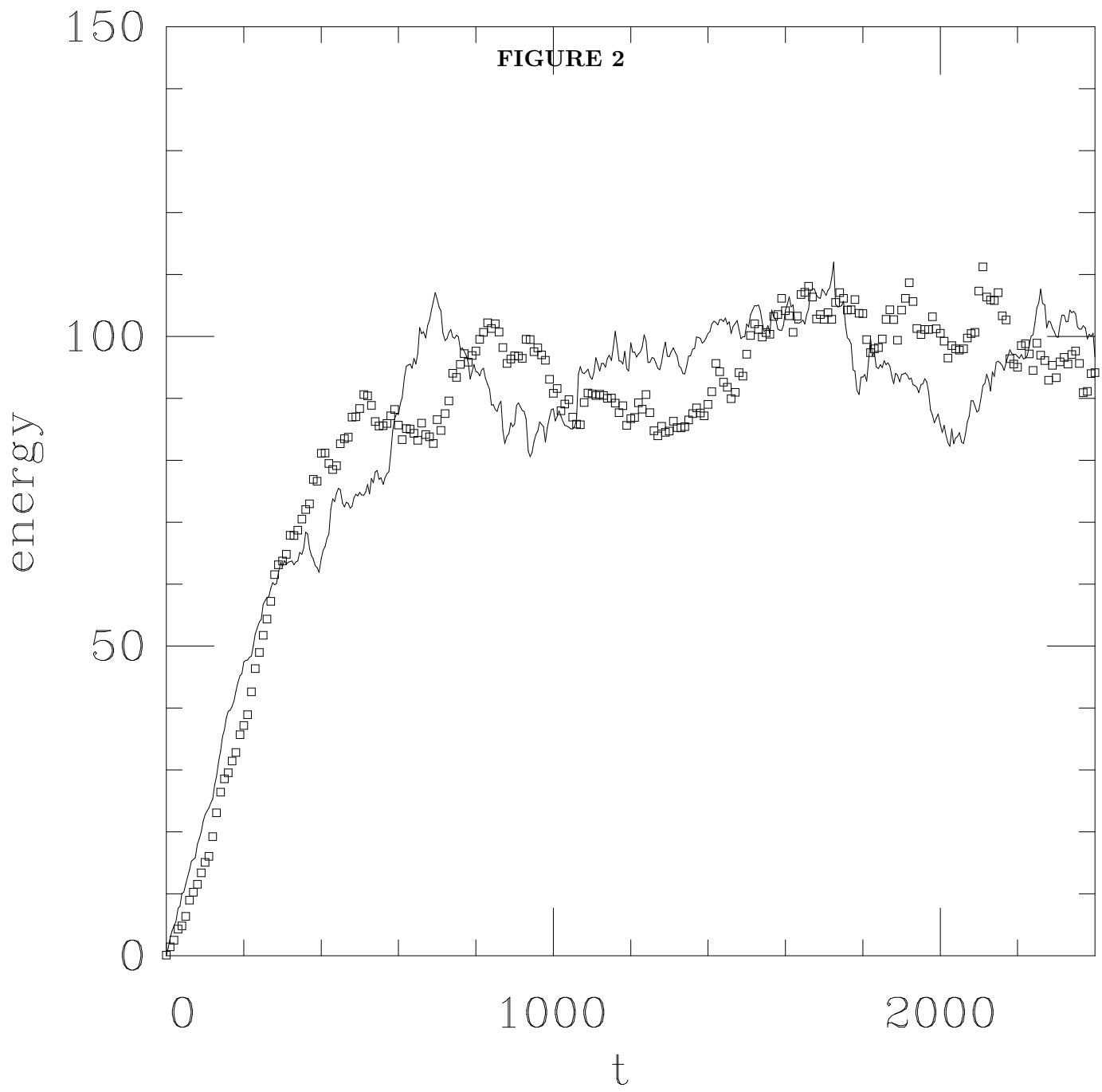
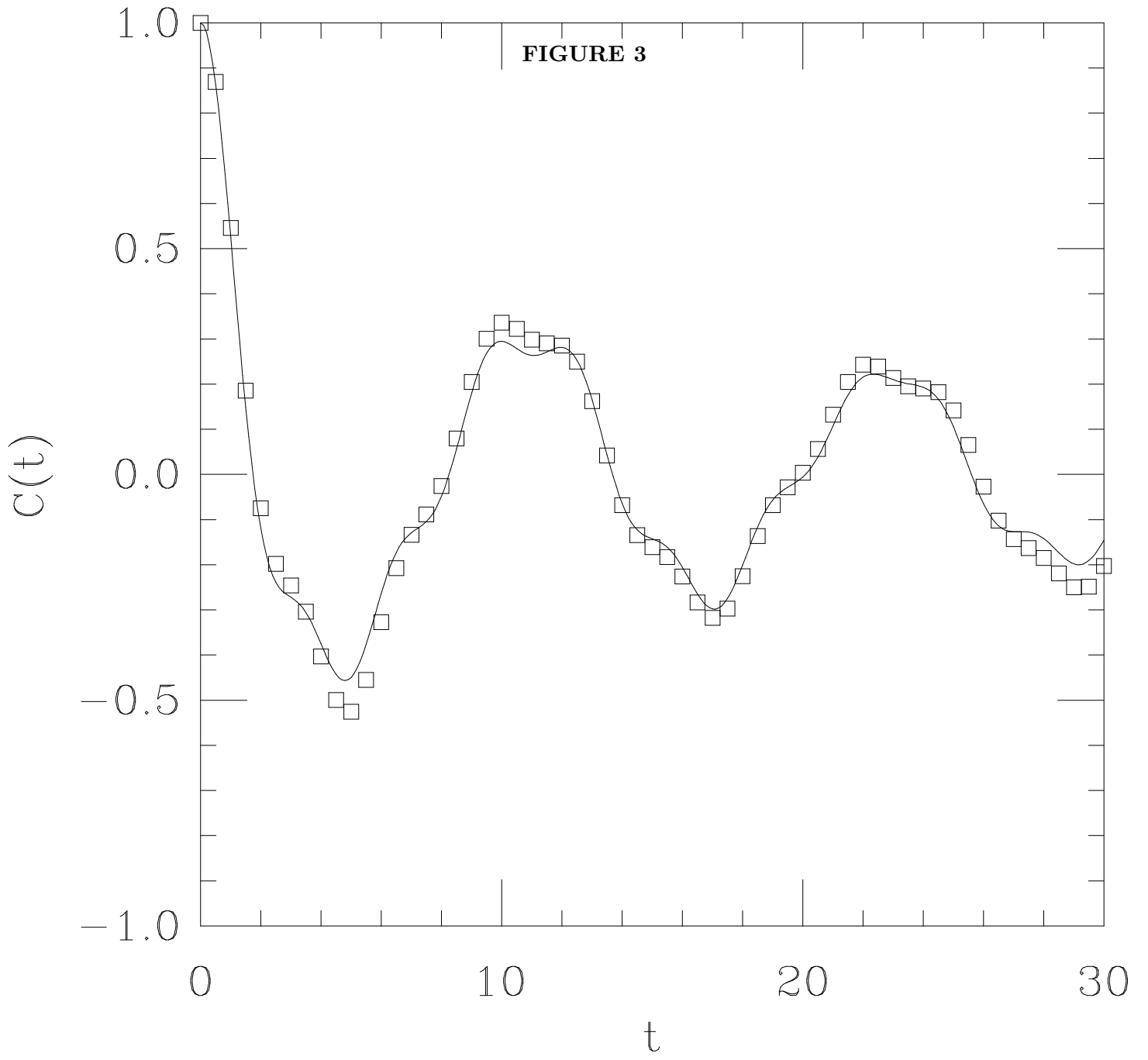
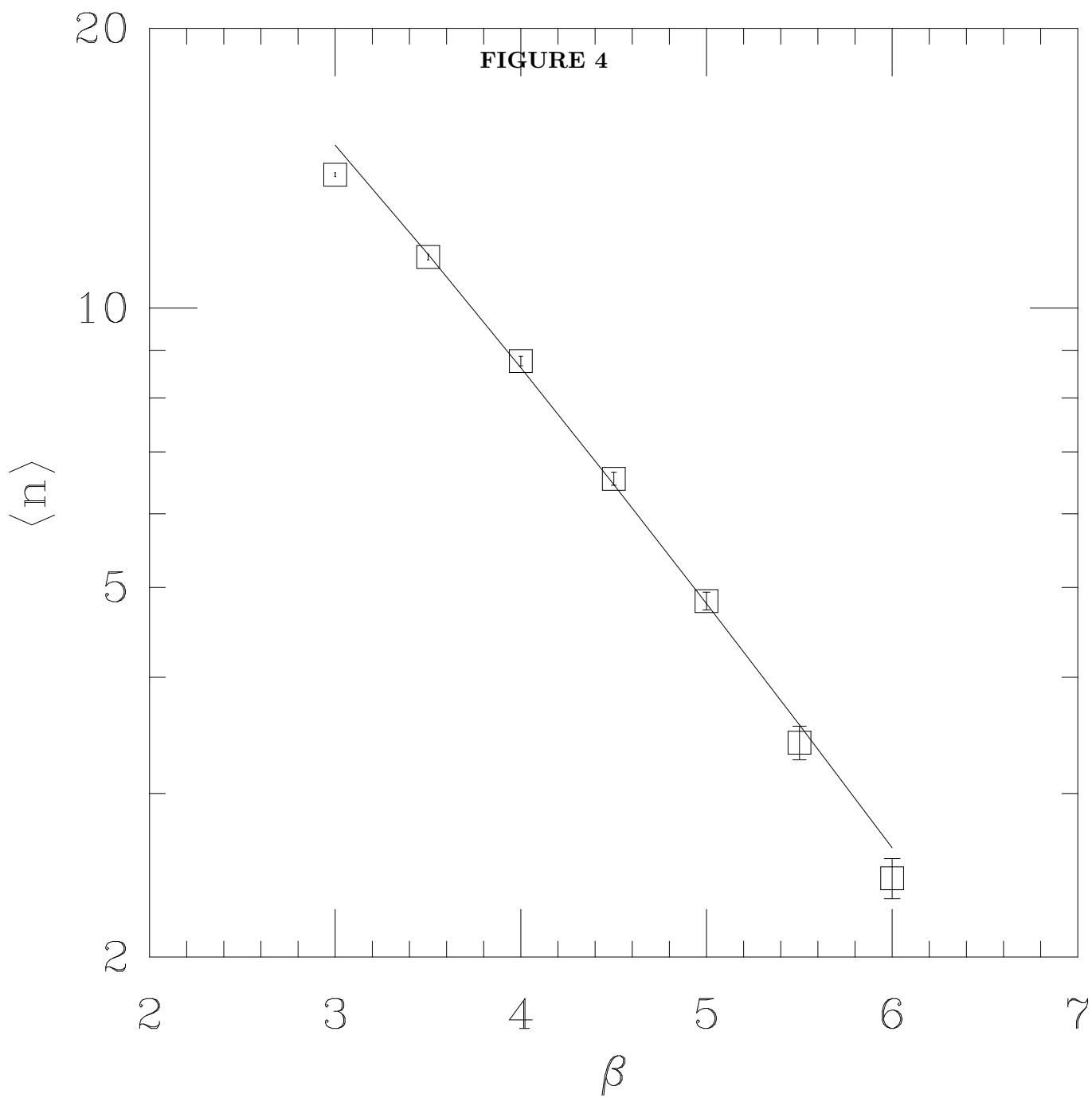
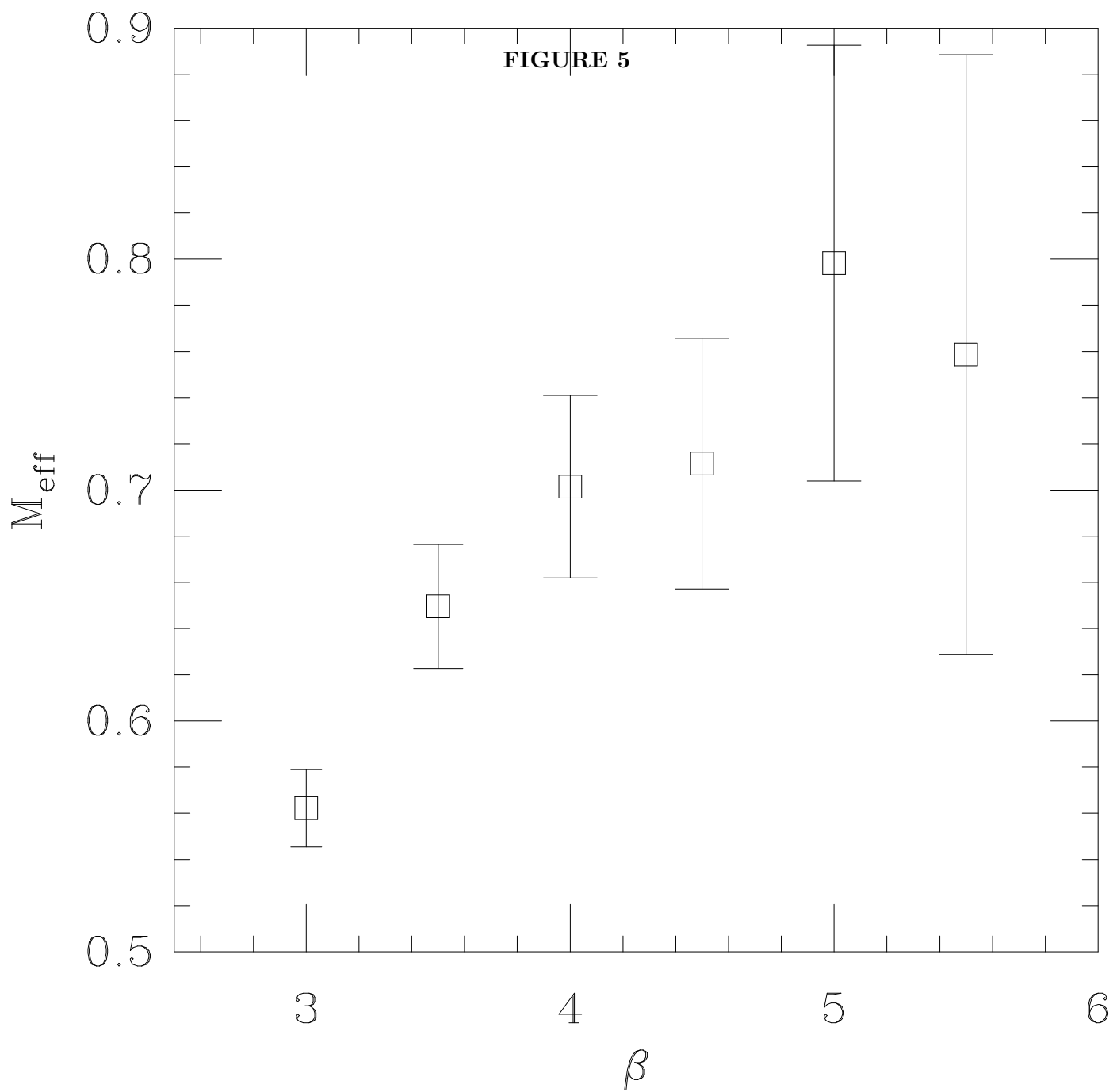


FIGURE 3







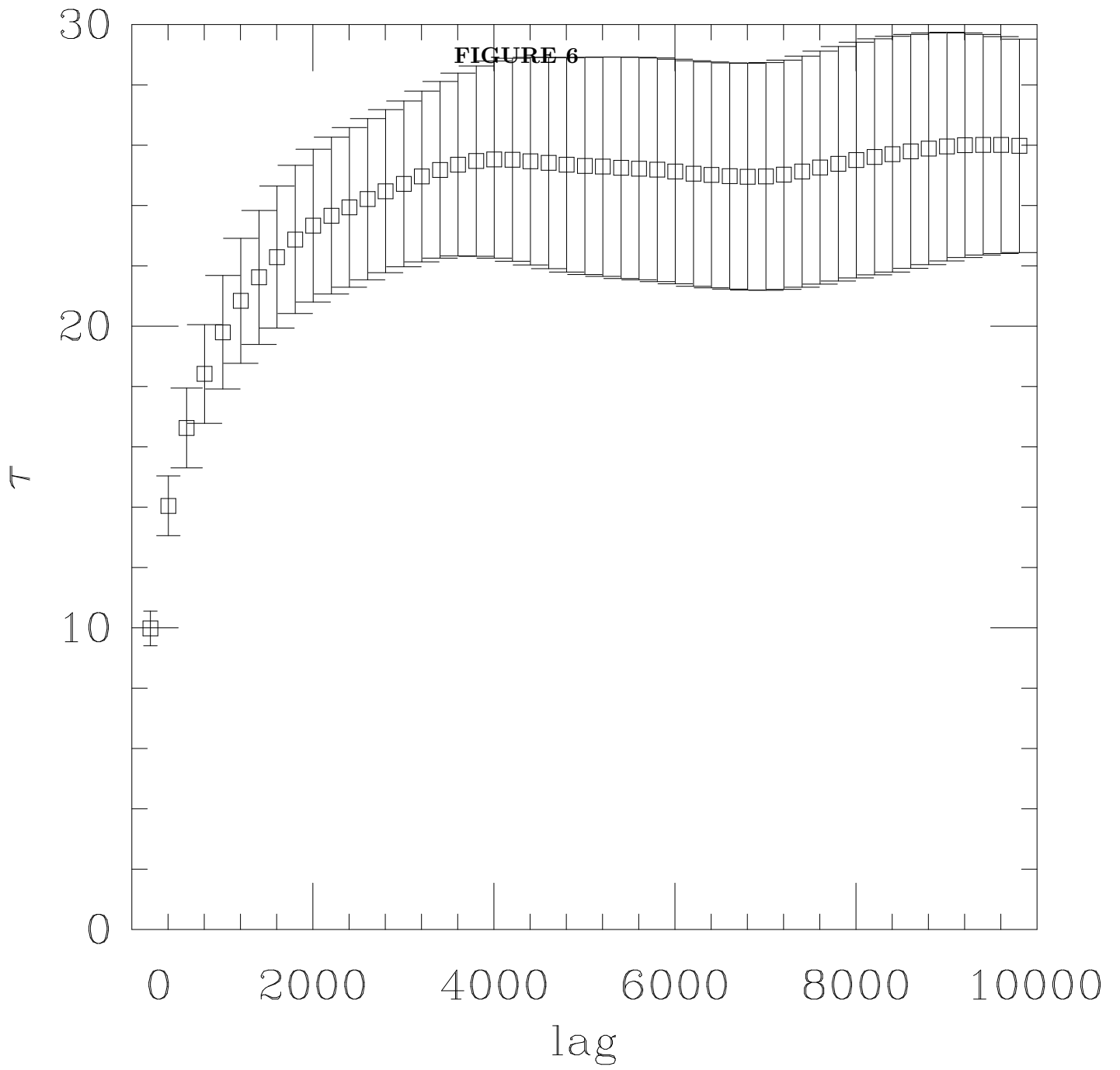


FIGURE 7

